

Arsenate and arsenite removal by Fe-modified activated carbon supported nano-TiO₂: influence factors and adsorption effect

F. X. Qin^{1,2}, C. F. Wei^{1*}, Z. K. Wang³, G. Li², X. L. Li², Y. J. Li²

¹ College of Resources and Environment, Southwest University, Chongqing 400716, China;

² Key Laboratory for Information System of Mountainous Areas and Protection of Ecological Environment of Guizhou Province, Guizhou Normal University, Guiyang 550001, China;

³ College of Eco-Environmental Engineering, Guizhou Minzu University, Guiyang, 550025, China

Received December 18, 2017, Revised January 26, 2018

In this paper, the preparation of Fe-modified activated carbon supported nano-TiO₂ (Fe-TiO₂/AC) particles and the test results of the properties of the synthesized material, including crystallinity structure, surface morphology, functional groups, and surface texture, obtained using X-ray diffraction, transmission electron microscopy, scanning electron microscopy, and Fourier transform infrared spectroscopy, are presented. The removal rates of arsenic were evaluated using batch tests under several simulated conditions, including pH, ionic strength, material dosage, and initial arsenic concentration. The results indicated that arsenic removal was effective in weak alkaline conditions, and the maximum adsorption for arsenic was observed at pH = 8. The arsenic removal rate was improved by increasing the ionic strength and the adsorbent dosage. The adsorption of As(III) and As(V) reached equilibrium within 3 h and 1.14 h, respectively. The pseudo-second-order model satisfactorily described the adsorption processes. Isotherm data were fitted using the Freundlich equation. The isotherm results showed that the maximum adsorption capacities of Fe-TiO₂/AC were 28.66 mg·g⁻¹ for As(III) and 35.22 mg·g⁻¹ for As(V). In the adsorption process, nano-TiO₂ and Fe₂O₃ played key roles in increasing the adsorption efficiency and converting As(III) to As(V). Moreover, the presence of Fe(III) accelerated the oxidation of arsenic.

Keywords: Fe-TiO₂/AC, Arsenic removal, Adsorption, Redox, Chemical characterization.

INTRODUCTION

Arsenic (As) is a metalloid, which exists in the form of As(III) and As(V) [1,2] and can be widely detected in both natural and anthropogenic sources [3]. Serious health threats for humans and other living organisms have attracted considerable attention because of their high toxicity [4,5]. From the perspective of natural pollution, both As(III) and As(V) are found in soil, organisms, and water, and are mobilized through a combination of natural processes such as rock weathering, biological activities, and volcanic emissions [6]. In the case of anthropogenic activities, arsenic contaminations were mainly caused by combustion of fossil fuels, petroleum refineries, mining, and nonferrous smelting activities [7-9]. In China, the living surroundings are exposed to different degrees of arsenic pollution; moreover, arsenic pollution exceeds its threshold level (10 µg·L⁻¹) in drinking water [10]. Therefore, effective removal of arsenic or conversion from As(III) to As(V) at the highest oxidation rate for the purpose of reducing its toxicity and other detrimental effects is a key issue in arsenic pollution control and treatment.

A large number of methods, including physical-chemical treatment processes such as precipitation,

ion-exchange, adsorption, and membrane filtration, have been used for removing toxic elements from water and, subsequently, for alleviating water pollution [10-16]. Among them, adsorption is one of the most preeminent removal methods because of its low cost, ease of operation, and high efficiency [17]. A higher efficiency of arsenic removal can be achieved by indirectly adsorbing arsenic or converting As(III) to As(V) through a pre-oxidation process, as As(III) is difficult to be removed directly by using most of the existing techniques.

Titanium dioxide [18] and its modified counterparts [19] exhibit excellent removal arsenic efficiency by adsorbing it from the polluted water. In brief, the adsorption can be attributed to their special physical and chemical properties, such as high theoretical adsorption capacity, large specific surface area, oxidation behavior, photo-catalytic efficiency, and high affinity of the surface hydroxyl groups [20]. In addition, the particle size of the adsorbent affects the adsorption capacity for arsenic [18]. Bang *et al.* [21] found that the arsenic species had a high affinity for the surface sites of TiO₂. Although TiO₂-doped materials exhibit excellent adsorption performance, the effective load amount may hinder an extensive use of traditionally prepared nano-TiO₂-doped materials. Long and Tu

*) To whom all correspondence should be sent:

E-mail: weicf@swu.edu.cn

© 2018 Bulgarian Academy of Sciences, Union of Chemists in Bulgaria

[22] studied arsenic removal by using activated-carbon-supported granular nano-TiO₂, but they found that the nano-TiO₂ loaded amount was too low to decrease the arsenic level. To improve the loaded amount of nano-TiO₂, tetrabutyl titanate doped with activated carbon powder was produced using the sol-gel method in our experiment. In addition, arsenic was adsorbed widely by iron compounds (granular ferric hydroxide and ferric oxide) and several common minerals such as goethite and ferrihydrite [23].

In this article, we have attempted to modify TiO₂-doped activated carbon powder using iron. Here, we have focused on whether the modification of supported TiO₂ can enhance its adsorption ability to arsenic by iron compounds. Thus, in this study, a new adsorbent was prepared and used to remove As(III) and As(V) from an aqueous solution. The effects of pH, adsorbent dosage, and ionic strength were elucidated to explore the optimum removal conditions. The adsorption kinetics and isotherms were investigated to probe the adsorption efficiency and the maximum adsorption capacity for arsenic. The main objectives of this research were as follows: (a) to produce a sufficient amount of a uniform adsorption material with preloaded TiO₂ and iron content, (b) to evaluate the arsenic adsorption by the material and determine its maximum adsorption capacity for As(III) and As(V), and (c) to explain the adsorption mechanism of the material.

EXPERIMENTAL

Materials

Nitric acid (HNO₃), anhydrous ethanol (C₂H₅OH), tetrabutyl titanate (C₁₆H₃₆O₄Ti), and glacial acetic acid (CH₃COOH) were purchased from Sinopharm Chemical Reagent Co., Ltd (China). Ammonium sulfate [(NH₄)₂SO₄, analytical reagent] was supplied by Tianjin Kermel Chemical Reagent Co., Ltd. (China). Activated carbon powder was obtained from Hunan Deban Activated Carbon Co., Ltd. (China). NaAsO₂ was the source for preparing 1000 mg·L⁻¹ of As(III). 1000 mg·L⁻¹ of As(V) was prepared by the oxidation of a stock solution of As(III) using excess potassium peroxydisulfate (K₂S₂O₈). The NaCl, NaOH (0.1 mol·L⁻¹), and HCl (0.1 mol·L⁻¹) solutions were prepared using deionized water (18.2 MΩ·cm). Stock solutions were stored in dark before the experiments. Unless otherwise stated, all chemicals were of analytical grade and above.

Fe-TiO₂/AC powder preparation

The preparation of the adsorbent powder is described in detail in [24]. In brief, the procedure

was as follows: 16.4 g of the activated carbon powder was pre-soaked in HNO₃ and then, added to a mixture of 70 mL anhydrous C₂H₅OH and 20 mL tetrabutyl titanate at a pH of 2–3 (adjusted using glacial acetic acid) to obtain solution A. Next, 20 mL of anhydrous ethanol (C₂H₅OH), 60 mL of water, 2.4 g of ammonium sulfate [(NH₄)₂SO₄], and ferric nitrate were mixed in a clean breaker; the mixture was stirred continuously by using a magnetic stirrer. Then, acetic acid (CH₃COOH) was used to regulate the pH in the range of 2–3, resulting in the mixed solution B. Solution B was dropped slowly to mix with solution A using a speed stirring process (200 rpm), and the resulting mixture was continuously stirred by using a magnetic mixer at 400 rpm at room temperature (25–28°C) for 2 h. Further, the Fe-TiO₂/AC soliquid was produced as follows: The Fe-TiO₂/AC sol was rested for 24 h and then, smoothly ground after drying at 100°C. The resulting powder was roasted in a covered crucible in a muffle furnace at 500°C for 2 h and then, naturally cooled down to room temperature. The result was Fe-TiO₂/AC powder.

Material characterization

The new material was characterized using X-ray diffraction (XRD), transmission electron microscopy/scanning electron microscopy (TEM/SEM), and Fourier transform infrared spectroscopy (FTIR) methods. The XRD (DY2862, Holland) method was used to explore the crystal structure of the material. TEM (JEM-2100F, Japan) and SEM (JSM-6490LV, Japan) were used for determining the shapes of the adsorbent. The functional groups of the adsorbent were observed using FTIR (TENSOR27, Bruker, Germany). The titanium content and the iron content were determined using ICP-OES (Optima 5300V, Perkin Elmer, America), and the TiO₂ loaded amount was calculated.

Batch adsorption experiments

All glassware and polyethylene bottles were soaked in 10% HNO₃ for at least 24 h before each experiment and then, washed thrice with distilled water and dried in an oven. NaCl was used to adjust the ionic strength of the solution, and HCl and NaOH (both 0.1 mol·L⁻¹) were used for the required pH adjustment. The pH values were measured using a pH meter (3E, Shanghai Leici Inc., China). 1000 mg·L⁻¹ of As(III) and As(V) solution was diluted to obtain the required concentrations. The reaction volume was selected to be 25 mL, and the adsorbent was added in the appropriate dosage and at the appropriate time at room temperature

F.X. Qin et al.: Arsenate and arsenite removal by Fe-modified activated carbon supported nano-TiO₂ ... (25–28°C) and settled for 20 min. The sample was then centrifuged for 30 min (4000 rpm), and equilibrium arsenic solution was moved into sample vials and analyzed using atomic fluorescence spectrometry (AFS 933, Beijing Titan Instruments Co., Ltd., China) and inductively coupled plasma optical emission spectroscopy (ICP-OES, Optima 5300V, PerkinElmer, America). The effects of pH, ionic strength, adsorbent dosage, and time were evaluated. All of the adsorption samples were shaken continuously and uniformly in the oscillator (HY-5, Changzhou Huanyu Scientific Instrument Factory, China). The resulting solution samples were analyzed within 24 h.

Adsorption results calculations

The arsenic removal rate and the amount of arsenic adsorbed on the manufactured materials were calculated using equations (1) and (2):

$$\text{Arsenic removal rate(\%)} = \frac{c_1 - c_2}{c_1} \times 100 \quad (1)$$

Adsorption capacity by a unit mass of adsorbent

$$\text{As/adsorbent(mg g}^{-1}\text{)} = \frac{(c_1 - c_2) \times V}{M} \quad (2)$$

where C_1 is the initial arsenic concentration ($\text{mg}\cdot\text{L}^{-1}$), C_2 is the arsenic concentration after adsorption ($\text{mg}\cdot\text{L}^{-1}$), V is the solution volume (L), and M is the adsorbent dosage (g).

Adsorption kinetic test

Two kinetic models, namely the pseudo-first-order kinetic model and the pseudo-second-order kinetic model, were used to fit the experimental data in order to estimate the adsorption rate.

The form of the pseudo-first-order kinetic model is as follows [25]:

$$\frac{dQ_t}{dt} = K_1(Q_e - Q_t) \quad (3)$$

The following is its linear equation:

$$\ln(Q_e - Q_t) = \ln Q_e - \ln K_1 - K_1 t \quad (4)$$

The pseudo-second-order kinetic model can be expressed as follows [25]:

$$\frac{dQ_t}{dt} = K_2(Q_e - Q_t)^2 \quad (5)$$

Its linear equation is as follows:

$$\frac{t}{Q_t} = \frac{1}{K_2 Q_e^2} + \frac{t}{Q_e} \quad (6)$$

where Q_e is the amount of adsorbed arsenic at the adsorption equilibrium ($\text{mg}\cdot\text{g}^{-1}$); Q_t is the amount of adsorbed arsenic at a certain point of time t ($\text{mg}\cdot\text{g}^{-1}$); K_1 and K_2 are the adsorption rate constants of the pseudo-first-order kinetic model (h^{-1}) and the pseudo-second-order kinetic model, respectively; and t is the adsorption time (h). K_1 is calculated by fitting a straight line equation of $\ln(Q_e - Q_t) - t$, and the reaction rate increases with an increase in K_1 . K_2 is calculated by fitting the straight line equation of $\frac{t}{Q_t}$ and t .

Adsorption isothermal test

The Langmuir and Freundlich isotherm equations can be expressed as follows [26]:

Langmuir equation:

$$\frac{C_e}{Q_e} = \frac{C_e}{Q_m} + \frac{t}{K_L Q_m} \quad (7)$$

Freundlich equation:

$$\lg(Q_e) = \lg(K_F) + \frac{1}{n} \lg(C_e) \quad (8)$$

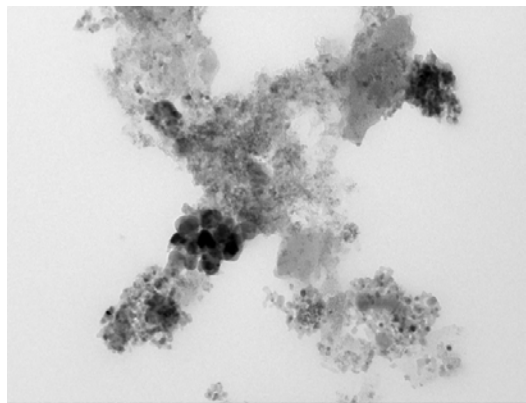
where Q_e is the amount of adsorbed arsenic at the adsorption equilibrium ($\text{mg}\cdot\text{g}^{-1}$), C_e is the arsenic concentration at the adsorption equilibrium ($\text{mg}\cdot\text{L}^{-1}$), Q_m is the calculated constant related to the adsorption capacity ($\text{mg}\cdot\text{g}^{-1}$), K_L is the Langmuir adsorption equilibrium constant related to the affinity of the binding sites and the adsorption heat, K_F is the Freundlich constant, and n is a parameter related to the adsorption strength. Large values of K_F and n indicated better adsorption performance of the adsorbent.

RESULTS AND DISCUSSION

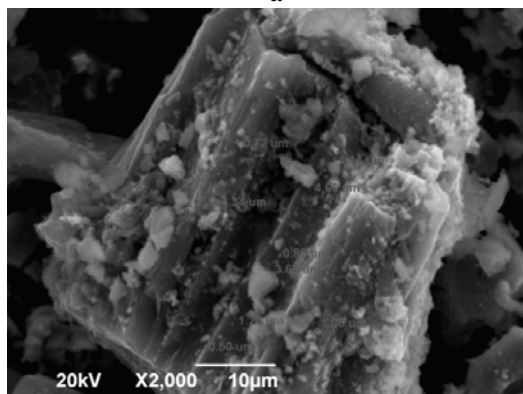
Characterization of Fe-TiO₂/AC

For the characterization of the Fe-TiO₂/AC powder, we initially examined the prepared Fe-TiO₂/AC sample using TEM and SEM, as shown in Fig. 1. Fig. 1(a) shows the presence of a dense microstructure. The powdered activated carbon and nano-TiO₂ or Fe₂O₃ particles were interlaced. We observed that the powder was an irregular ellipsoid with many filamentous network chains around it. Further, we inferred that the irregular ellipsoid was nano-TiO₂ and the black particles in the external network chain were Fe₂O₃. Fig. 1(a) also shows that particles of different sizes were wrapped around each other. We observed amorphous particles, microcrystalline particles, and nanocrystalline particles. Thus, we concluded that the adsorption channels of the material had stacking-capillary

pores formed by the accumulation of nanoparticles [27]. Fig. 1(b) shows that some of the nano-TiO₂ and Fe₂O₃ particles attached to the surface of the activated carbon and a small number of particles entered into the channels of the activated carbon. The supported particles exhibited a variety of particle sizes.



a



b

Fig. 1. TEM and SEM images of the TiO₂/AC sample: TEM and (b) SEM;

On the basis of these observations and the TEM results for the material, we concluded that supported nano-TiO₂ with relatively large particles was produced by agglomeration of small nano-TiO₂ particles. The average particle size of the adsorbent was around 10 – 52 nm.

The FTIR spectrum of the material is shown in Fig. 2. This figure shows that the broad characteristic band at 3418.22 cm⁻¹ is assigned to the O-H stretching vibration [19]. At around 1640 cm⁻¹, a free water molecule H-O-H bending vibration was discovered [28]. The bending vibration at 1100 cm⁻¹ belonged to the hydroxyl groups on the surface of the metal oxides [29]. The broad wavenumber range of around 550 – 800 cm⁻¹ was attributed to the characteristic bands of the Ti-

O-Ti bond [30]. The band of 570 cm⁻¹ belonged to the Fe-O bond.

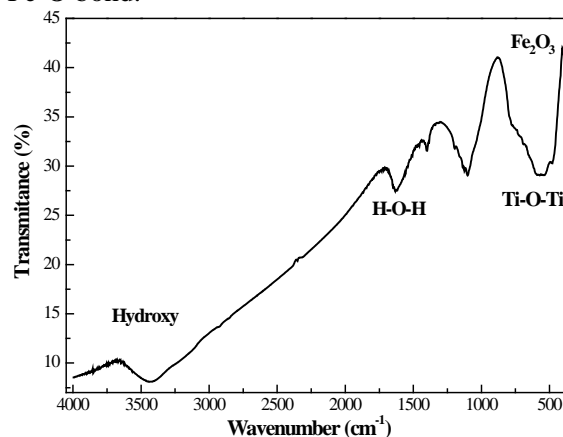


Fig. 2. FTIR spectrum of TiO₂/AC

The prepared material particles were exposed to an XRD test. As shown in Fig. 3, the diffraction peaks of the material were at 25.51°, 37.82°, 48.13°, 53.92°, and 75.13°, which showed a good consistency with the diffraction structure of TiO₂. Further, according to the JCPDS standard card (No.71-1167), the crystal form of TiO₂ was anatase [31]. The peak at 2θ = 26.6° matched with the characteristic diffraction peak of SiO₂. The Fe-TiO₂/AC particles included a considerable proportion of hematite-Fe₂O₃, because the diffraction peaks of Fe-TiO₂/AC were observed at 33.52°, 35.92°, 49.81°, and 54.01°, which were assigned to the diffraction of Fe₂O₃ and the peak structure was more obvious as the Fe(III) doping improved the crystallinity of the adsorbent.

Using this technique, we determined the concentration of TiO₂ and Fe₂O₃ to be 250 and 114 mg·g⁻¹, respectively. Furthermore, we demonstrated that the supported TiO₂ species were particularly stable under acidic conditions, as no leached TiO₂ was detected following a treatment with aqua regia (5 vol%).

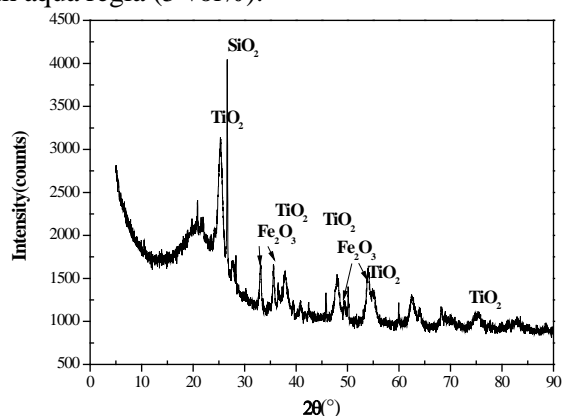


Fig. 3. XRD pattern of the TiO₂/AC

pH is an important influencing factor for the arsenic removal process [32]. The surface charges of the adsorbent and the arsenic compound forms are influenced by pH variation, thus affecting the arsenic adsorption [33].

The effect of pH on As(III) and As(V) removal was determined at pH values ranging from 3 to 11. Fig. 4 shows that arsenic adsorption was strongly influenced by pH. The arsenic removal rate and the amount of adsorbed arsenic increased with an increase in pH and then decreased until pH = 11. The removal rate of As(V) gradually increased from 90.88% to 99.00% when the solution pH increased from 3 to 8, and then, rapidly decreased from 99.00% to 82.39% with an increase in pH from 8 to 11. The amounts of adsorbed As(V) increased from 0.038 to 0.409 mg·g⁻¹ and then, decreased to 0.035 mg·g⁻¹ on the Fe-TiO₂/AC particles. A similar As(V) adsorption behavior by P25 [34] and ferric hydroxides [35] was reported earlier. The amount of As(III) adsorbed onto the Fe-TiO₂/AC particles increased steadily from 0.028 to 0.034 mg·g⁻¹ at pH values of 3–8 and then, declined gradually to 0.029 mg·g⁻¹.

The increasing removal rate and amount of As(V) adsorbed resulted from a progressive competition between the arsenate and hydroxyl anions for titanium bonding and iron bonding when pH increased from 3 to 8. The arsenic removal rate and the amount of arsenic adsorbed onto Fe-TiO₂/AC reached a maximum at pH = 8, which was attributed to the fact that arsenic combines more easily with titanium and iron in a weakly alkaline medium where arsenic is mainly present in anion forms such as AsO₃³⁻, HAsO₃²⁻, H₂AsO₃⁻, and HAsO₄²⁻, and the nano-TiO₂ surface has a positive charge; here, the uptake of arsenic is rapid because of the repulsion from its surface at pH values higher than 8 [36].

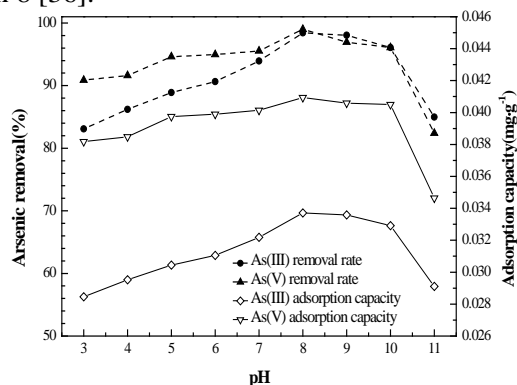


Fig.4. Effect of pH on arsenic removal at room temperature under the following conditions: initial concentration of As(III) 70 µg·L⁻¹ and As(V) 84 µg·L⁻¹, solution volume 25 mL, adsorbent dosage 0.05 g, and ionic strength 0.01 mol·L⁻¹

Note that more As(V) than As(III) was removed because H₂AsO₄⁻ and HAsO₄²⁻ are the primary As(V) forms observed at pH 3–11. Therefore, the As(V) removal results were possibly caused by the interaction between the neutralization of the anionic and the positive charges. As(III) is mainly present as H₃AsO₃, which remains as a neutral molecule in a non-alkaline environment. However, in a weakly alkaline environment, H₃AsO₃ is gradually transformed into anionic H₂AsO₃⁻ because of the protonation effect and the surface of nano-TiO₂ produced more adsorption sites with positive charges by removing hydroxyl ions; thus, more As(III) was adsorbed [37].

When pH > 8, the removal rate and the amount of adsorbed arsenic decreased because of the decrease in the proportion of the positive charges on the adsorbent surface [36] and the competitive adsorption of OH⁻ and arsenic compounds; we expected to achieve arsenic desorption in strongly acidic or alkaline solutions. Note that the As(III) removal by FeCl₃ decreased with an increase in the pH value from 9 to 10 and depended primarily on the incomplete precipitation of Fe(III) and then on the repulsion between H₂AsO₃⁻ and negatively charged iron hydroxide flocs [38]. The trend of the As(III) removal rate and the amount of As(III) adsorbed onto Fe-TiO₂/AC showed a sharp decrease at pH values of 10–11 and was consistent with the adsorption of anions of the weak acid on the oxide-water interface [23]. We also proved that the adsorbent was a combination of iron oxides and titanium because this phenomenon was observed in the case of iron (hydr)oxides [35] and titanium dioxide-adsorbed As(III) [39]. The finding that the removal rate and the adsorbed amount of As(III) onto Fe-TiO₂/AC were more favorable than those of As(V) at pH values of 8–11 [36,40] was attributed to the following two reasons: (a) changes in the form of the As(III) compound (from H₃AsO₃ to H₂AsO₃⁻) and (b) the initial concentration difference. Qiao *et al.* [38] observed the same difference: the As(V) removal was more favorable than the As(III) removal at a lower pH, but the opposite trend was observed at higher pH values. From pH 4 to 11, the adsorption efficiency of As(V) and As(III) was similar because of the photocatalytic oxidation of TiO₂ in the presence of dissolved oxygen and light [41]. In addition, the surface potential of metal oxides became more negative and considerable adsorption of As(V) and As(III) was observed when pH > point of zero charge (PZC), which indicated that the arsenic species were adsorbed on TiO₂ through surface complexation and not through electrostatic interactions [21,41]. The results of the present study revealed that pH 8 was the optimal adsorption condition for removing arsenic.

The removal rate and the amount of arsenic adsorbed onto Fe-TiO₂/AC as functions of the initial arsenic concentration are illustrated in Fig. 5 at the optimal pH. The arsenic removal rate decreased with an increase in the initial concentration. The amount of adsorbed arsenic increased because of the incomplete combination of the adsorption sites with arsenic and the inability of the adsorbed arsenic to reach saturation at a low initial arsenic concentration. In addition, a higher amount of As(V) than As(III) was adsorbed under the simulated operating conditions. The As(III) removal rate decreased continuously from 98.62% to 54.99% when the initial concentration increased to 10 mg·L⁻¹ and significantly declined at the initial concentration of 0.05–2 mg·L⁻¹; thereafter, the downward trend appeared to be gentle at the initial concentration of 2–10 mg·L⁻¹ and the amount of As(III) adsorbed onto Fe-TiO₂/AC increased from 0.023 to 2.674 mg·g⁻¹ with an obvious increase at the initial concentration of 1–10 mg·L⁻¹. As(V) displayed similar variation trends. The removal rate decreased from 99.12% to 65.9% when the initial concentration increased to 10 mg·L⁻¹, and the amount of As(V) adsorbed onto the Fe-TiO₂/AC particles increased from 0.026 to 3.259 mg·g⁻¹. The As(V) removal rate decreased sharply at the initial concentration of 0.05–5 mg·L⁻¹ and then, remained almost constant, and the adsorption amount of As(V) onto Fe-TiO₂/AC exhibited an obvious increase at the initial concentration of 1–10 mg·L⁻¹.

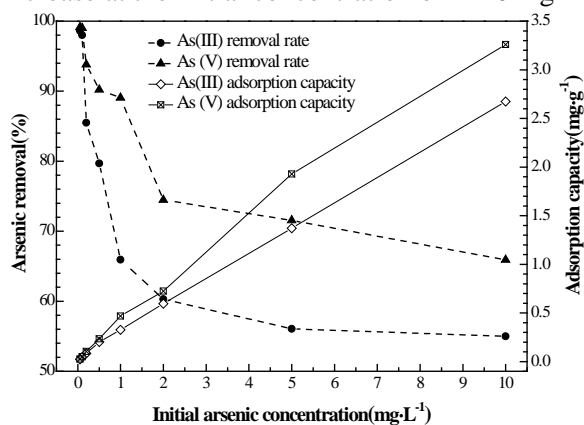


Fig.5. Effect of initial concentration on arsenic removal at room temperature under the following reaction conditions: pH = 8, solution volume 25 mL, adsorbent dosage 0.05 g, and ionic strength 0.01 mol·L⁻¹

Effect of the adsorbent dosage

The effect of the adsorbent dosage on the removal result is shown in Fig. 6. This figure shows that the As(III) and As(V) removal efficiencies are strongly influenced by the adsorbent dosage: 0.5 g

dosage was sufficient to reach the adsorption equilibrium when the initial arsenic concentration was 1.3 mg·L⁻¹, and Fe-TiO₂/AC was significantly efficient with respect to As(V) adsorption as compared to As(III) adsorption at an equivalent adsorbent level. The removal rate of arsenic increased with an increase in the adsorbent dosage, but the amount of adsorbed arsenic decreased. Further, a steep change occurred when the adsorbent dosage increased from 0.01 to 0.5 g, and a constant removal result was maintained with a further increase in the adsorbent dosage in the adsorption process. When 0.5 g of Fe-TiO₂/AC was added to 25 mL of an arsenic solution, more than 93% of As(V) and 95% of As(III) were adsorbed, but the amounts of As(V) and As(III) adsorbed were 0.055 mg·g⁻¹ and 0.065 mg·g⁻¹, respectively. The amount of arsenic adsorption decreased with an increase in the adsorbent dosage. When the dosage was less than 0.5 g, the amount of adsorbed arsenic sharply decreased and then reached equilibrium. Thus, we concluded that a higher adsorbent dosage resulted in a higher removal rate and a lower adsorption amount before the adsorption equilibrium was reached because the number of adsorption sites for the removal of arsenic increased with an increase in the adsorbent dosage and led to a higher removal rate, but the arsenic concentration remained unchanged in the adsorption process. The adsorption equilibrium was reached when the adsorbent dosage was 0.5 g. More adsorption sites were produced when the adsorbent dosage increased from 0.5 to 3.0 g, but these adsorption sites could not be fully utilized, which continued to keep arsenic adsorption capacity onto the adsorbent. Genç-fuhrman *et al.* [42] observed a similar phenomenon during arsenate removal from water by using neutralized red mud.

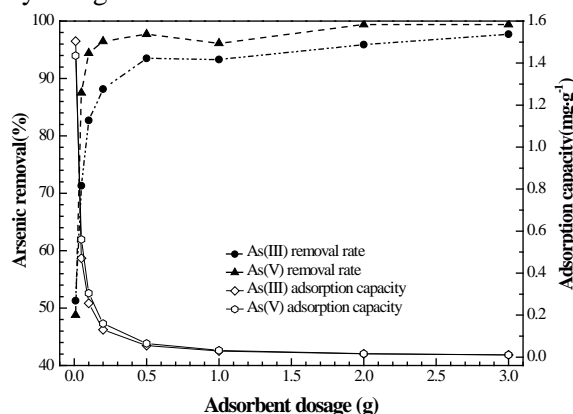


Fig.6. Effect of adsorbent dosage on arsenic removal at room temperature under the following reaction conditions: pH = 8, initial As concentration 1.3 mg·L⁻¹, solution volume 25 mL, and ionic strength 0.01 mol·L⁻¹

Effect of ionic strength

In this section, the removal rate of arsenic onto Fe-TiO₂/AC is discussed, and the results are shown in Fig. 7. As(III) adsorption was clearly more dependent on ionic strength than As(V) adsorption. In the adsorption process, the arsenic removal efficiency increased when the ionic strength increased to 0.5 mol·L⁻¹. The removal rate of As(III) increased from 89.71% to 94.70%. The amount of As(III) adsorbed onto Fe-TiO₂/AC increased from 0.058 to 0.061 mg·g⁻¹. Further, the removal rate of As(V) increased from 93.83% to 97.47%. The amount of As(V) adsorbed onto Fe-TiO₂/AC increased from 0.061 to 0.063 mg·g⁻¹ with an increase in the ionic strength. This was attributed to the linking of the surface hydroxyls of the adsorbent and arsenic by a ligand exchange reaction and the formation of inner surface complexes [43].

Adsorption kinetics

Adsorption kinetics experiments were conducted to determine the rate of arsenic removal. In this process, As(III) and As(V) removal by the material was conducted under the same conditions. The experimental results are presented in Fig. 8. It shows that arsenic removal rate was enhanced with increasing adsorption time before adsorption equilibrium was reached. The arsenic removal rate increased at a quick pace. The As(V) removal rate remains relatively constant within 70 min (1.17 h) to 1440 min (24 h) by the material under the current experimental conditions. In other words, the adsorption of As(V) reached equilibrium in 70 min (1.17 h). For As(III), adsorption equilibrium was attained in 90 min (1.5 h).

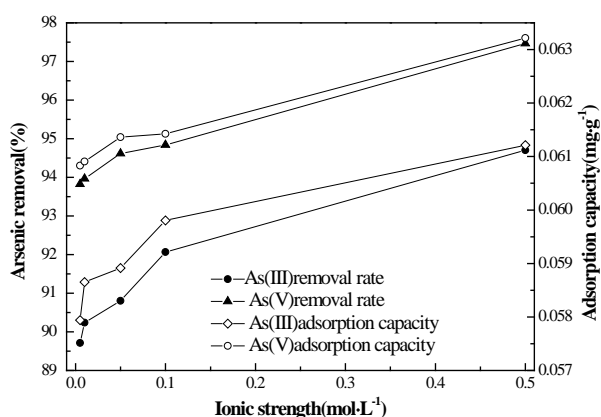


Fig.7. Effect of ionic strength on arsenic removal at room temperature under the following reaction conditions: pH = 8, initial As concentration 1.3 mg·L⁻¹, solution volume 25 mL, and adsorbent dosage 0.5 g

The kinetic parameters of the adsorption obtained using equation (4) are shown in Table 1. The correlation coefficients of the As(V) and As(III) adsorption were 0.7854 and 0.7835, respectively. The pseudo-first-order

kinetic model was used to describe the experimental data of As(V) and As(III) in the current conditions, but it failed to explain the arsenic adsorption onto Fe-TiO₂/AC. Therefore, we concluded that physical adsorption could not be ignored in the arsenic removal process, which implied that the adsorption rate of As(V) onto the adsorbent was faster than that of As(III). The experimental data were consistent with the information reflected by the K_f value.

The pseudo-second-order kinetic parameters are presented in Table 2. The data regarding the As(III) and As(V) adsorption onto the adsorbent were well described by the pseudo-second-order model. The obtained correlation coefficients were higher than 0.9999 and were in the following order: As(V) > As(III). K_2 followed the order As(V) > As(III).

As compared to the pseudo-first-order model, the pseudo-second-order model fitted the experimental data very well, which implied that the arsenic adsorption onto the adsorbent was a complex process involving surface adsorption, inter-components, and intra-particle diffusion [44]. An excellent effect of arsenic adsorption onto the adsorbent was obtained using physical adsorption and chemical adsorption, and chemical bonds were the main factors influencing the chemical adsorption process [45].

Adsorption isotherms

The adsorption isotherm experiments were performed at different initial concentrations ranging from 0.2 to 562.1 mg·L⁻¹. The adsorption equilibrium time was maintained at 3 h for the As(III) removal and 70 min for the As(V) removal.

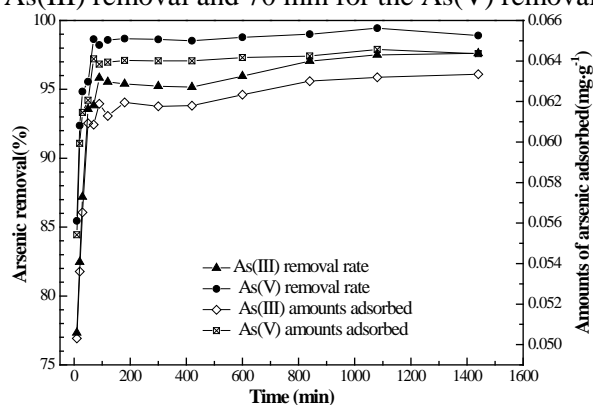


Fig.8. Kinetic curve of arsenic removal by the adsorbent at room temperature under the following reaction conditions: pH = 8, initial As concentration 1.3 mg·L⁻¹, solution volume 25 mL, and adsorbent dosage 0.5 g

Table 1. Pseudo-first-order parameters and equation for As(III) and As(V) removal

Parameters	As(III)	As(V)
K_f	1.6405	2.1026
R^2	0.7835	0.7854
Fitting equation	$\ln(Q_e - Q_t) = -1.641t - 4.551$	$\ln(Q_e - Q_t) = -2.103t - 4.648$

Table 2. Pseudo-second-order parameters and equation for As(III) and As(V) removal

Parameters	As(III)	As(V)
K_2	212.8190	581.9038
R^2	0.99996	0.99999
Fitting equation	$t/Q_t = 15.776t + 1.170$	$t/Q_t = 15.511t + 0.413$

The Freundlich and Langmuir parameters are presented in Table 3 and Table 4, respectively. These results indicated that the arsenic adsorption data fitted the Freundlich isotherm better than the Langmuir isotherm, and the corresponding good correlation coefficient values were between 0.9528 and 0.9780, which indicated that the arsenic adsorption by the material was heterogeneous adsorption on a non-uniform surface. The n value of the Freundlich equation was greater than 1; this indicated that the adsorption of arsenic was easy. The K_F value of As(V) was relatively large, which implied that the removal of As(V) was more favorable than that of As(III). According to the isotherm results, the maximum adsorption capacities of Fe-TiO₂/AC were 28.66 mg·g⁻¹ and 35.22 mg·g⁻¹ for As(III) and As(V), respectively. As compared to many other adsorbents, the new material exhibited excellent adsorption capacity. For instance, Pena *et al.* [41] found that 8.30 mg·g⁻¹ of As(III) and 11.20 mg·g⁻¹ of As(V) were removed by nanocrystalline TiO₂. Altundoğan *et al.* [46] estimated the maximum adsorption capacities of red mud for As(III) and As(V) to be 0.33 mg·g⁻¹ and 0.35 mg·g⁻¹, respectively.

Table 3. Freundlich isotherm constants

Parameters	As(III)	As(V)
K_F	0.3538	1.5172
R_2	0.9780	0.9528
n	1.4215	1.7184
Fitting equation	$\lg Q_e = -0.45119 + 0.70348 \lg C_e$	$\lg Q_e = 0.18103 + 0.58195 \lg C_e$

Table 4. Langmuir isotherm constants

Parameters	As(III)	As(V)
K_F	0.025	0.228
R_2	0.8824	0.8967
Q_m	14.63	16.71
Fitting equation	$C_e/Q_e = 0.0684C_e + 2.735$	$C_e/Q_e = 0.0598C_e + 0.263$

Adsorption mechanism

Arsenic removal from an aqueous solution by Fe-TiO₂/AC requires simultaneous physical and chemical adsorption. Further, a sufficient number of adsorption sites are required for arsenic removal. The positive charge on the TiO₂ surface facilitates arsenate adsorption by electrostatic interactions at pH = 8, where the arsenate is present mainly as anion. The deprotonation of arsenite may remove the hydroxyl ions from the coordinating layer of the TiO₂ support, and thus, some adsorption sites with a positive charge are created on the adsorbent surface

to adsorb the As(III) anions in the process [37]. A nano-TiO₂ loading can complete the partial conversion of As(III) to As(V) because the catalytic oxidation activity of TiO₂ and arsenic can form monodentate or bidentate complexes at the surface of TiO₂ [23,47]. In the adsorption process, As-O-AsO₄³⁻ and As-O-H₂AsO₄⁻ groups were formed during the As(V) removal by nano-TiO₂ with anatase crystals, and As-O-AsO₃³⁻ and As-O-HAsO₄²⁻ were found under mild conditions during the As(III) removal and the adsorption of As(V) and As(III) on TiO₂ by the As-O-Ti and As-O bonds [18]. The Fe(III) supports of the Fe-TiO₂/AC particles accelerated the oxidation of As(III) to As(V) [48]. Then, the arsenic anions and Fe-OH of Fe-TiO₂/AC formed bidentate or binuclear complexes [49,50]. Further, iron-modified activated carbon was effective in arsenic adsorption because the oxyanionic arsenic species were adsorbed at the iron oxyhydroxide surface by forming complexes with the surface sites [51]. Therefore, the adsorption mechanism of arsenic on Fe-TiO₂/AC was mainly influenced by the complex formation.

CONCLUSIONS

Fe-TiO₂/AC powder was synthesized using the sol-gel method; it was mesoporous and had a particle size ranging in nanometers. Further, it had a high adsorption capacity for arsenic in a weakly alkaline solution, and the maximum adsorption capacity of the material was observed at pH = 8. An increased amount of arsenic was adsorbed by increasing the ionic strength, material dosage, and initial arsenic concentration. The adsorbent was better at removing As(V) than at removing As(III). The adsorption kinetics and the adsorption isotherms were described well by the pseudo-second-order kinetic equation and the Freundlich isotherm model, respectively. Further, the arsenic adsorption equilibrium by the adsorbent was reached within 3 h.

Acknowledgement: The authors would like to express their sincere gratitude for the financial support from National Natural Science Foundation (21467005) and Science and Technology Department from Guizhou Province [LH(2014)7383 and (2016)1071], and the Student's Platform for Innovation and Entrepreneurship Training Program (201510672003).

REFERENCES

1. J.F. Ferguson, J. Gavis, *Water Res.*, **6**(11), 1259 (1972).
2. Y. Wu, X.Y. Zhou, M. Lei, J. Yang, J. Ma, P.W. Qiao, T.P. Chen., *Appl. Geochem.*, **77**, 44 (2017).
3. M. Yu, *Aus. J. Chem.*, **67**(5), 813 (2014).
4. M. Tuzen, K.O. Saygi, I. Karaman, M. Soylak, *Food Chem. Toxicol.*, **48**(1), 41 (2010).

5. T. Luo, J. Yu, *J. Resid. Sci. Technol.*, **12**, S17 (2015).
6. P.L. Smedley, D.G. Kinniburgh, *Applied Geochem.*, **17**(5), 517 (2002).
7. B.A. Manning, S. Goldberg, *Environ. Sci. Technol.*, **31**(7), 2005 (1997).
8. M. Berg, H.C. Tran, T.C. Nguyen, H.V. Pham, R. Schertenleib, A.W. Giger, *Environ. Sci. Technol.*, **35**(13), 2621 (2001).
9. M.L. Pierce, C.B. Moore, *Environ. Sci. Technol.*, **14**(2), 214 (1980).
10. G. Yu, D. Sun, Y. Zheng, *Environ. Health Persp.*, **115**(4), 636 (2007).
11. F. Fu, Q. Wang, *J. Environ. Manage.*, **92**(3), 407 (2011).
12. A. Dabrowski, Z. Hubicki, P. Podkościelny, E. Robens, *Chemosphere*, **56**(2), 91 (2004).
13. G. Yan, T. Viraraghavan, *Water Res.*, **37**(18), 4486 (2003).
14. G. Chen, *Sep. Purif. Technol.*, **38**(1), 11 (2004).
15. T.A. Kurniawan, G.Y.S. Chan, W.H. Lo, S. Babel, *Chem. Eng. J.*, **118**(1–2), 83 (2006).
16. D. Mohan, P.C. Jr, *J Hazard. Mater.*, **142**(1–2), 1 (2007).
17. A. Demirbas, *J. Hazard. Mater.*, **157**(2–3), 220 (2008).
18. L. Ma, S. Tu, *Environ. Chem. Lett.*, **9**(4), 465 (2011).
19. T.S. Anirudhan, L. Divya, J. Parvathy, *J. Chem. Technol. Biot.*, **88**(5), 878 (2013).
20. H. Cao, B. Li, J. Zhang, F. Lian, X. Kong, M. Qu, *J. Mater. Chem.*, **22**(19), 9759 (2012).
21. S. Bang, M. Patel, L. Lippincott, X. Meng, *Chemosphere*, **60**(3), 389 (2005).
22. X. Long, S. Tu, *Indust. Water Treat.*, **32**(4), 29 (2012).
23. M. Pena, X. Meng, G.P. Korfiatis, C. Jing, *Environ. Sci. Technol.*, **40**(4), 1257 (2006).
24. L.I. Rong, X. Xiao, C. Wang, *Mater. Rev.*, **25**, 68 (2011).
25. P. Pillewan, S. Mukherjee, T. Roychowdhury, S. Das, A. Bansawal, S. Rayalu, *J. Hazard. Mater.*, **186**(1), 367 (2011).
26. X. Fan, D.J. Parker, M.D. Smith, *Water Res.*, **37**(20), 4929 (2003).
27. A. Manceau, *Geochim. Cosmochim. Acta*, **59**(17), 3647 (1995).
28. Y. Guo, Z. Zhu, Y. Qiu, J. Zhao, *Environ. Sci.*, **25**(5), 944 (2013).
29. Z.J. Li, S.B. Deng, G. Yu, J. Huang, C. Lim, *Chem. Eng. J.*, **161**(1), 106 (2010).
30. S. Abbasizadeh, A.R. Keshtkar, M.A. Mousavian, *J. Ind. Eng. Chem.*, **20**(4), 1656 (2014).
31. I.R. Bellobono, A. Carrara, B. Barni, A. Gazzotti, *J. Photoch Photobiol. A.*, **84**(1), 83 (1994).
32. S. Bekkouche, S. Baup, M. Bouhelassa, S. MolinaBoisseau, C. Petrier, *Desalin. Water Treat.*, **37**(1–3), 364 (2012).
33. L. Zhang, Y. Zhu, H. Li, N. Liu, X. Liu, X. Guo, *Rare Metals*, **29**(1), 16 (2010).
34. H. Lee, W. Choi, *Environ. Sci. Technol.*, **36**(17), 3872 (2002).
35. X. Meng, S. Bang, G.P. Korfiatis, *Water Res.*, **34**(4), 1255 (2000).
36. T.F. Lin, J.K. Wu, *Water Res.*, **35**(8), 2049 (2001).
37. P.K. Dutta, A.K. Ray, V.K. Sharma, F.J. Millero, *J. Colloid. Interf. Sci.*, **278**(2), 270 (2004).
38. J. Qiao, Z. Jiang, B. Sun, Y. Sun, Q. Wang, X. Guan, *Sep. Purif. Technol.*, **92**(1), 106 (2012).
39. D. Xie, L. Cao, J. Cui, *Chin. J. Environ. Eng.*, **7**(4), 1279 (2013). (In Chinese).
40. X. P. Yan, R. Kerrich, M. J. Hendry, *Geochim. Cosmochim. Acta*, **64**(15), 2637 (2000).
41. M. E. Pena, G.P. Korfiatis, M. Patel, L. Lippincott, X. Meng, *Water Res.*, **39**(11), 2327 (2005).
42. H. Genç-Fuhrman, J.C. Tjell, D. Mcconchie, *J. Colloid Interf. Sci.*, **264**(2), 327 (2003).
43. Z. J. Wu, H.N. Liu, H.F. Zhang, *Environ. Chem.*, **29**(6), 997 (2010).
44. U. Farooq, J.A. Kozinski, M.A. Khan, M. Athar, *Bioresource Technol.*, **101**(14), 5043 (2010).
45. Y.S. Ho, *Water Res.*, **40**(1), 119 (2006).
46. H.S. Altundoğan, S. Altundoğan, F. Tümen, M. Bildik, *Waste Manage.*, **20**(8), 761 (2000).
47. G. He, M. Zhang, G. Pan, *J. Phys. Chem. C.*, **113**(52), 21679 (2009).
48. P. Mondal, C. Balomajumder, B. Mohanty, *J Hazard. Mater.*, **144**(1), 420 (2007).
49. B.A. Manning, S.E. Fendorf, S. Goldberg, *Environ. Sci. Technol.*, **32**(16), 2383 (1998).
50. S.D. And, J.G. Hering, *Environ. Sci. Technol.*, **37**(18), 4182 (2003).
51. W. Chen, R. Parette, J. Zou, F.S. Cannon, B.A. Dempsey, *Water Res.*, **41**(9), 1851 (2007).

ИЗВЛИЧАНЕ НА АРСЕНАТ И АРСЕНИТ С ПОМОЩТА НА НАНО-TiO₂, НАНЕСЕН ВЪРХУ МОДИФИЦИРАН С ЖЕЛЯЗО АКТИВЕН ВЪГЛЕН: ВЛИЯЕЩИ ФАКТОРИ И АДСОРБЦИОНЕН ЕФЕКТ

Ф. Кин^{1,2}, Ч. Уей^{1,*}, Ж. Уанг³, Г. Ли², Кс. Ли², И. Ли²

¹ Колеж по ресурси и околна среда, Югозападен университет, Чонгкинг 400716, Китай

² Лаборатория по информационни системи за планински области и опазване на околната среда на провинция Гуижоу, Университет на Гуижоу, Гуянг 550001, Китай

³ Колеж по екоинженерство, Университет на ГуижоуМинци, Гуянг, 550025, Китай

Постъпила на 18 декември 2017, Коригирана на 26 януари 2018

(Резюме)

В статията е представено получаването на нано-TiO₂, нанесен върху активен въглен, модифициран с желязо (Fe-TiO₂/AC), както и резултатите от изпитването на свойствата на материала, включително кристална структура, повърхностна морфология, функционални групи и повърхностна текстура. Резултатите са получени с помощта на рентгенова дифракция, трансмисионна електронна микроскопия, сканираща електронна микроскопия и Fourier трансформираща инфрачервена спектроскопия. Степента на извличане на арсена е оценена чрез статични експерименти при симулирани условия на рН, йонна сила, количество адсорбент и изходна концентрация на арсена. Установено е, че извличането на арсена протича ефективно в слабоалкална среда и максимална адсорбция се наблюдава при рН 8. Извличането на арсена се подобрява при повишаване на йонната сила и количеството адсорбент. Адсорбцията на As(III) и As(V) достига равновесие съответно за 3 ч и 1.14 ч. Моделът от псевдотори порядък описва задоволително адсорбционните процеси. Експерименталните данни съответстват на уравнението на Freundlich. Изотермичните резултати показват, че максималният адсорбционен капацитет на Fe-TiO₂/AC е 28.66 mg·g⁻¹ за As(III) и 35.22 mg·g⁻¹ за As(V). Нано-TiO₂ и Fe₂O₃ играят ключови роли за повишаване на адсорбционната способност и превръщането на As(III) в As(V). Наличието на Fe(III) ускорява окислението на арсена.